vPIF-1 is an insulin-like antiferroptotic viral peptide

Belavgeni, Alexia ; Maremonti, Francesca ; Tonnus, Wulf ; Stadtmüller, Marlena ; Gavali, Shubhangi ; Mallais, Melodie ; Flade, Karolin ; Brucker, Anne ; Becker, Jorunn Naila ; Beer, Kristina ; Tmava, Mirela ; Stumpf, Julian ; Gembardt, Florian ; Hugo, Christian ; Giacca, Mauro ; Hale, Benjamin G ; Perakakis, Nikolaos ; Sha, Wei ; Pratt, Derek A ; Schally, Andrew V ; Bornstein, Stefan R ; Linkermann, Andreas

Abstract: Iridoviridae, such as the lymphocystis disease virus-1 (LCDV-1) and other viruses, encode viral insulin-like peptides (VILPs) which are capable of triggering insulin receptors (IRs) and insulin-like growth factor receptors. The homology of VILPs includes highly conserved disulfide bridges. However, the binding affinities to IRs were reported to be 200- to 500-fold less effective compared to the endogenous ligands. We therefore speculated that these peptides also have noninsulin functions. Here, we report that the LCDV-1 VILP can function as a potent and highly specific inhibitor of ferroptosis. Induction of cell death by the ferroptosis inducers erastin, RSL3, FIN56, and FINO2 and nonferroptotic necrosis produced by the thioredoxin-reductase inhibitor ferroptocide were potently prevented by LCDV-1, while human insulin had no effect. Fas-induced apoptosis, necroptosis, mitotane-induced cell death and growth hormone-releasing hormone antagonist-induced necrosis were unaffected, suggesting the specificity to ferroptosis inhibition by the LCDV-1 VILP. Mechanistically, we identified the viral C-peptide to be required for inhibition of lipid peroxidation and ferroptosis inhibition, while the human C-peptide exhibited no antiferroptotic properties. In addition, the deletion of the viral C-peptide abolishes radical trapping activity in cell-free systems. We conclude that iridoviridae, through the expression of insulin-like viral peptides, are capable of preventing ferroptosis. In analogy to the viral mitochondrial inhibitor of apoptosis and the viral inhibitor of RIP activation (vIRA) that prevents necroptosis, we rename the LCDV-1 VILP a viral peptide inhibitor of ferroptosis-1. Finally, our findings indicate that ferroptosis may function as a viral defense mechanism in lower organisms.

DOI: https://doi.org/10.1073/pnas.2300320120

Schally, Andrew V; Bornstein, Stefan R; Linkermann, Andreas (2023). vPIF-1 is an insulin-like antiferroptotic viral peptide. Proceedings of the National Academy of Sciences of the United States of America, 120(21):e2300320120. DOI: https://doi.org/10.1073/pnas.2300320120

PNAS RESEARCH ARTICLE | MEDICAL SCIENCES

vPIF-1 is an insulin-like antiferroptotic viral peptide

Alexia Belavgeni[a], Francesca Maremonti[a], Wulf Tonnus[a], Marlena Stadtmüller[a], Shubhangi Gavali[a], Melodie Mallais[b], Karolin Flade[a], Anne Brucker[a], Jorunn Naila Becker[a], Kristina Beer[a], Mirela Tmava[a], Julian Stumpf[a], Florian Gembardt[a], Christian Hugo[a], Mauro Giacca[c], Benjamin G. Hale[d], Nikolaos Perakakis[e], Wei Sha[f,g,h,i,j], Derek A. Pratt[b], Andrew V. Schally[f,g,h,i,j,1], Stefan R. Bornstein[a,k,l,m,n,1], and Andreas Linkermann[a,o,1]

Contributed by Andrew V. Schally; received January 6, 2023; accepted April 19, 2023; reviewed by Ilse S. Daehn, Scott J. Dixon, and Bradlee Heckman

Iridoviridae, such as the lymphocystis disease virus-1 (LCDV-1) and other viruses, encode viral insulin–like peptides (VILPs) which are capable of triggering insulin receptors (IRs) and insulin-like growth factor receptors. The homology of VILPs includes highly conserved disulfide bridges. However, the binding affinities to IRs were reported to be 200- to 500-fold less effective compared to the endogenous ligands. We therefore speculated that these peptides also have noninsulin functions. Here, we report that the LCDV-1 VILP can function as a potent and highly specific inhibitor of ferroptosis. Induction of cell death by the ferroptosis inducers erastin, RSL3, FIN56, and FINO2 and nonferroptotic necrosis produced by the thioredoxin-reductase inhibitor ferroptocide were potently prevented by LCDV-1, while human insulin had no effect. Fas-induced apoptosis, necroptosis, mitotane-induced cell death and growth hormone–releasing hormone antagonist–induced necrosis were unaffected, suggesting the specificity to ferroptosis inhibition by the LCDV-1 VILP. Mechanistically, we identified the viral C-peptide to be required for inhibition of lipid peroxidation and ferroptosis inhibition, while the human C-peptide exhibited no antiferroptotic properties. In addition, the deletion of the viral C-peptide abolishes radical trapping activity in cell-free systems. We conclude that iridoviridae, through the expression of insulin-like viral peptides, are capable of preventing ferroptosis. In analogy to the viral mitochondrial inhibitor of apoptosis and the viral inhibitor of RIP activation (vIRA) that prevents necroptosis, we rename the LCDV-1 VILP a viral peptide inhibitor of ferroptosis-1. Finally, our findings indicate that ferroptosis may function as a viral defense mechanism in lower organisms.

regulated necrosis | ferroptosis | viral defense | necroptosis | apoptosis

Significance

Ferroptosis is a clinically important failsafe event that contributes to cell death in diseases such as Alzheimer's disease, stroke, myocardial infarction, and acute kidney injury. A physiological role of ferroptosis, however, has not been identified. Here, we show that fish viruses can express an insulin-like peptide that functions as a potent inhibitor of ferroptosis, indicating that virally infected cells evade ferroptosis in lower organisms. The antiferroptotic properties of the molecule, which we refer to as viral peptide inhibitor of ferroptosis-1 (vPIF-1), require a functional region that is known as the C-peptide. This report identifies a virally encoded protein that inhibits ferroptosis.

Iridoviridae were recently reported to express viral insulin/insulin–like growth factor (IGF)1-like peptides (VILPs) as examples of the first recognized viral hormones (1–4). These VILPs share up to 50% homology with human insulin/IGF-1 and are found in blood and fecal samples of humans (1, 3). The best studied examples of VILPs are those expressed by lymphocystis disease virus-1 (LCDV-1), lymphocystis disease virus-Sa, grouper iridovirus, and Singapore grouper iridovirus (SGIV) (1–3, 5). In each one of these virally expressed proteins, all the six critical cysteine residues are conserved. These residues form intra- and interchain disulfide bonds that are required for the tertiary protein structure of insulins. However, the binding to the human insulin receptors (IRs) and IGF-receptor was 200- to 500-fold less potent compared to human insulin (1, 3). Its potential role as a natural competitive antagonist of the human IGF-1 receptor (6) was discussed in detail recently, and was suggested to function even as a natural antagonist of IGF-1 receptor signaling (7). However, it remains unclear why antagonizing the IGF-1 receptor should be beneficial for viral replication. While IR in mammals controls metabolism, the IR–like gene daf-2 of *Caenorhabditis elegans* predominately functions to provide stress resistance (8). Therefore, we hypothesized that hormone-independent functions of VILPs may allow viral escape from host defense in lower organisms. A central mechanism of host defense is the induction of regulated cell death (RCD), but this, to the best of our knowledge, has not been tested for IR.

Signaling pathways of RCD have evolved in the course of evolution as host defense pathways. Known RCD pathways comprise apoptosis (9), necroptosis (10), pyroptosis (11), ferroptosis (12), and death induced by inhibitors of the growth hormone–releasing hormone (GHRH) (13). While intracellular bacteria are controlled by an inflammasome-mediated RCD referred to as pyroptosis (14), viruses are controlled by apoptosis and necroptosis. Viruses have evolved several countermeasures to escape apoptosis and necroptosis (15). Viral caspase inhibitors such as crmA (16), viral antiapoptotic BCL2-like suppressors such as Vmia (17, 18), and rip homotypic interaction motif-containing proteins such as M45 (19) are prominent examples. Although it was studied in detail over the last decade (20), a (patho-)physiological role for ferroptosis, yet another form of regulated necrosis, remains elusive (12, 21).

Author contributions: A. Belavgeni, C.H., M.G., B.G.H., N.P., D.A.P., S.R.B., and A.L. designed research; A. Belavgeni, F.M., W.T., M.S., S.G., M.M., K.F., A. Brucker, J.N.B., K.B., M.T., and F.G. performed research; W.S. and A.V.S. contributed new reagents/analytic tools; A. Belavgeni, F.M., W.T., M.S., S.G., K.F., A. Brucker, J.N.B., K.B., J.S., C.H., M.G., B.G.H., N.P., A.V.S., S.R.B., and A.L. analyzed data; and A.L. wrote the paper.

Reviewers: I.S.D., Icahn School of Medicine at Mount Sinai; S.J.D., Stanford University; and B.H., Department of Molecular Medicine, USF Morsani College of Medicine.

Competing interest statement: A.V.S. and S.R.B. hold patents on MIA602. A.V.S. patents are assigned to the University of Miami and VA. Other authors declare no competing interest regarding any of the presented data in this manuscript.

[1]To whom correspondence may be addressed. Email: andrew.schally@va.gov, stefan.bornstein@uniklinikum-dresden.de, or Andreas.Linkermann@uniklinikum-dresden.de.

This article contains supporting information online at https://www.pnas.org/lookup/suppl/doi:10.1073/pnas.2300320120/-/DCSupplemental.

Published May 15, 2023.

Here, we demonstrate that the iridovirus LCDV-1-encoded VILP, but not human insulin, functions as a potent inhibitor of ferroptosis, while other host defense cell death pathways, such as apoptosis and necroptosis, are not affected by the presence of this molecule. We therefore name this molecule the viral peptide inhibitor of ferroptosis-1 (vPIF-1). The antiferroptotic function of vPIF-1 depends on a short C peptide-like domain, but the human C peptide did not affect ferroptosis. We find that vPIF-1 has radical trapping antioxidant (RTA) activity, enabling it to inhibit lipid peroxidation. Finally, we demonstrate that the viral resistance to ferroptosis can be overcome by GHRH inhibitor–induced necrosis. These data suggest the existence of a previously unrecognized host defense strategy against viruses by inhibiting ferroptosis through VILPs.

Results

Iridoviridae (Fig. 1*A*) express insulin-like peptides, such as the LCDV-1 insulin–like peptide (commonly referred to as LCDV-1, herein referred as vPIF-1). We investigated vPIF-1 in classical ferroptosis assays. Therein, HT1080 cells were treated with a covalent inhibitor of the glutathione reductase 4 (GPX4), the major inhibitor of ferroptosis-inducing lipid peroxidation. The proferroptotic function of this inhibitor, RSL3, is known to be inhibited by the first-in-class ferroptosis inhibitor ferrostatin-1 (Fer-1), a RTA that prevents ferroptosis downstream of GPX4 inhibition (22). We used the vital dye 7AAD and a marker of phosphatidylserine exposure (annexin V) as a standard readout, with combined positivity as a marker for necrotic cell death. As demonstrated in Fig. 1*B*, more than 80% of control cells exhibited double negativity in this assay. 1.13 μM RSL3, as expected, killed more than 80% of HT1080 cells in this assay within 4 h of incubation, resulting in a reduction of double-negative cells to 18%, and Fer-1, as expected, reversed this effect. Addition of increasing concentrations (100 nM to 1 μM) of vPIF-1 protected HT1080 cells from RSL3-induced ferroptosis as efficiently as 1 μM Fer-1, and the combined treatment with 1 μM LCDV-1 and Fer-1 provided no significant additional protection. In an independent approach, ferroptosis following 4 h of RSL3 treatment was entirely reversed by LCDV-1, while 1 μM of human insulin provided no protection in this assay (Fig. 1*C*). Biological replicates of these experiments were repeated at least three times and a quantification is presented in Fig. 1*C* (right plot). Similar results were obtained in the highly ferroptosis-sensitive adrenocortical carcinoma cell line NCI-H295R upon 2-h RSL3 treatment including coincubation with vPIF-1 and Fer-1 (*SI Appendix*, Fig. S1*A*). Structurally, human and iridoviridae-encoded insulin-like peptides are similar in their a and b chains which include disulfide bonds. However, significant structural differences between the C-peptides are present. The viral C-peptide contains 10 amino acids, while the human counterpart comprises a significantly longer amino acid chain (*SI Appendix*, Fig. S1*B*). We therefore hypothesized that the C-peptide of vPIF-1 might be required for the antiferroptotic activity. Thus, a derivative of vPIF-1 that lacks the C-peptide (referred throughout the entire manuscript as DesC-vPIF-1) was investigated alongside with vPIF-1, human insulin, and the human C-peptide in a 24-, 48-, and 72-h experiment of RSL3-induced ferroptosis in HT0180 cells. As for the protection control incubated with Fer-1, we found a vPIF-1-mediated protection of the cells upon RSL3 treatment for all the time points tested. In contrast, the DesC-vPIF-1, human insulin, and the human C-peptide failed to rescue the cells when challenged with RSL3 (Fig. 1*D*). These results suggest the antiferroptotic activity of vPIF-1 that depends on the viral C-peptide.

GHRH antagonists, such as MIA602, are known to kill the adrenocortical carcinoma cells, NCI-H295R, by necrosis, but no current treatment to prevent this form of cell death has been established. We therefore investigated the effects of vPIF-1 on 10 μM MIA602-induced necrosis. While 10 μM MIA602 effectively killed NCI-H295R cells, as previously reported (13), and ITS-1 addition accelerated this form of necrosis, vPIF-1 produced no nonspecific effect in this assay (*SI Appendix*, Fig. S1*C*). A simplified version of the VILPs in comparison to the human insulin and C-peptide is shown in Fig. 2*A*. The DesC-vPIF-1, insulin, and human C-peptide in NCI-H295R cells treated with MIA602 again exhibited no protection from necrosis (Fig. 2*B*). In addition, 10 μM MIA602 also caused cell death in NIH-3T3 cells (Fig. 2*C*). HT1080 cells showed increased positivity of annexin V/7AAD–stained cells at 20 μM of MIA602 (Fig. 2*D*). Therefore, we focused on NIH-3T3 cells to further investigate vPIF-1 and its mutant DesC-vPIF-1, alongside with human insulin and human C-peptide. Intriguingly, no protection from MIA602-induced necrosis was observed for any of the proteins in NCI-H295R cells (Fig. 2*E*). Previously, we reported that mitotane, an inducer of cell death in NCI-H295R cells and a drug for the treatment of patients with adrenocortical carcinomas, is independent of ferroptosis, but can be partially rescued by addition of a cell culture supplement (ITS-1) that contains polyunsaturated fatty acid alongside with human insulin, transferrin, and selenium (13). We therefore tested the effect of vPIF-1 on mitotane-induced cell death in NCI-H295R cells. In keeping with the hypothesis that vPIF-1 specifically inhibits ferroptosis, necrosis induced by 50 μM mitotane for 6 h was not reversed by vPIF-1 or human insulin, whereas ITS-1 exhibited partially protective effects (Fig. 2*F* and *SI Appendix*, Fig. S1*C*).

To test other modes of RCD, we expanded our investigations to apoptosis and necroptosis, two signaling pathways involved in host defense against virally infected cells. To induce apoptosis, we treated human Jurkat T cells with the extrinsic apoptosis-inducer Fas (also referred to as CD95 or Apo-1) and investigated phosphatidylserine exposure by annexin V positivity in flow cytometry. In contrast to 20 μM of the pancaspase inhibitor zVAD-fmk, vPIF-1, DesC-vPIF-1, human insulin, or the human C-peptide did not affect apoptosis (Fig. 3*A*). To investigate necroptosis, we treated human HT29 cells with 20 ng/mL recombinant human TNFα (tumor necrosis factor α), 1 μM of the SMAC (second mitochondrial-derived activators of caspases) mimetic birinapant, and 20 μM of the pancaspase inhibitor zVAD-fmk, collectively referred to as TSZ treatment for 6 h, an established protocol for induction of necroptosis (23). The receptor-interacting protein kinase 1 inhibitor necrostatin-1s (Nec-1s) served as a protection control. While Nec-1s reversed the sensitization of HT29 cells to necroptosis, vPIF-1, DesC-vPIF-1, human insulin, and the isolated human C-peptide had no effect in this assay (Fig. 3*B*). These data indicate that none of the known cell death pathways apart from ferroptosis are affected by vPIF-1, Des-vPIF-1, human insulin, or the human C-peptide.

We next tested the expression levels of human insulin receptor beta (IRβ) or the insulin-like growth factor receptor beta (IGF-IRβ) in a panel of different cell lines (human Jurkat T, human HT29, human NCI-H295R, human HT1080, and murine NIH-3T3 cells). Given the extraordinary sensitivity of renal tubules to GPX4-controlled ferroptosis (24–26), we additionally investigated the expression levels of IRβ and IGFR in freshly isolated renal tubules. As demonstrated in Fig. 3*C*, significant levels of expression of IRβ and IGF-IRβ were detectable in all lysates (apart from HT1080 cells that do not express IRβ), and a particularly high expression of IGF-IRβ was found in NIH-3T3 cells and murine freshly isolated tubules. It has been demonstrated that upon activation of the IRβ or the IGF-IRβ,

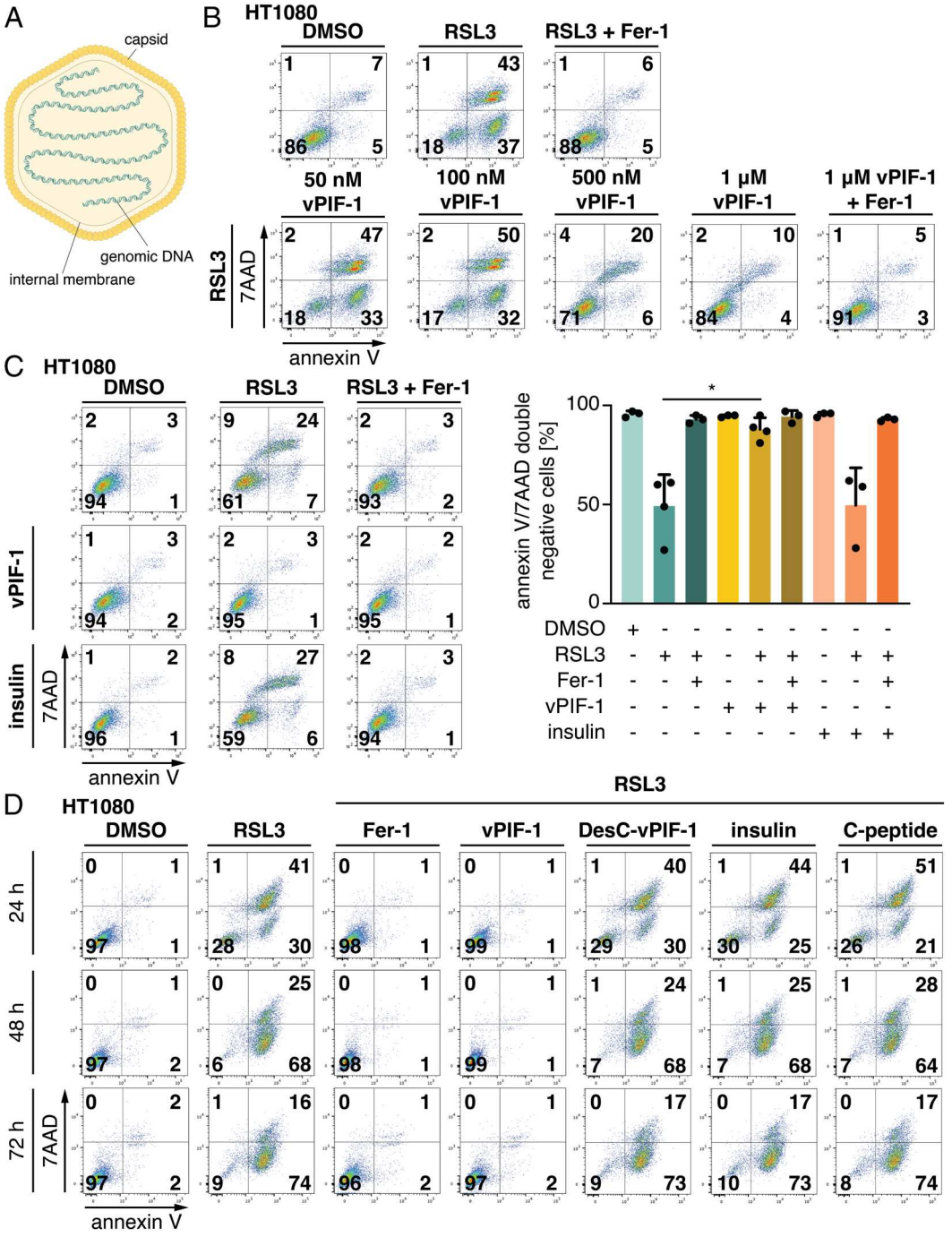

Fig. 1. The viral insulin, vPIF-1, inhibits type II ferroptosis. (*A*) Cartoon of the iridoviridae virus family. This illustration depicts a virion that has not been encapsulated in the membrane of the host cell. (*B*) HT1080 cells were used to undergo ferroptosis by the glutathione peroxidase 4 (GPX4) inhibitor, RSL3 (1.13 µM), for 4 h. Different concentrations of LCDV-1 were tested. Annexin V/7ADD positivity was assessed with FACS analysis. (*C*) HT1080 cells were treated with 1.13 µM RSL3 for 4 h, and 1 µM of vPIF-1 or human insulin was used to assess their effects on RSL3-induced ferroptosis. Fer-1 served as a protection control. Annexin V/7ADD positivity was assessed with FACS analysis. The bar graph shows the percentage of annexin V/7AAD double-negative cell repetitions of at least three independent experiments. Statistical analysis was performed using Student's *t* test for each sample. *$P \leqq 0.05$. (*D*) HT1080 cells were treated with 1.13 µM RSL3 for 24, 48, and 72 h. vPIF-1, DesC-vPIF-1 (the viral insulin lacking the C-peptide), human insulin, and the human C-peptide (1 µM) were used to assess their effect on RSL3-induced cell death in the HT1080 cells. Annexin V/7ADD positivity was assessed with FACS analysis. For all experiments, Fer-1 (1 µM) served as the protection control. All primary FACS data shown are representative examples of at least three independent experiments.

the protein Akt becomes phosphorylated (27). To test the potency of VILPs on Akt phosphorylation, we stimulated HT1080 cells with 1 µM vPIF-1 or insulin for different time points and performed western blotting for total Akt and phospho-Akt (p-Akt). Upon incubation of the cells with either vPIF-1 or human insulin, increased phosphorylation Akt was detected (Fig. 3*D* and *SI Appendix*, Fig. S2*A*). This experiment is in keeping with previous reports on IGF-IRβ stimulation by vPIF-1.

To control for potential effects of the viral peptides on proliferation of the HT1080 cells, we employed the CyQUANT kit that revealed less DNA concentration upon treatment with RSL3. While cotreatment with vPIF-1 and Fer-1 maintained proliferation upon RSL3 stimulation, DesC-vPIF-1, human insulin, and C-peptide failed to do so (*SI Appendix*, Fig. S2*B*). These data largely rule out a direct effect of the viral insulin derivatives on cell proliferation, suggesting that the demonstrated changes are to be explained by cell death.

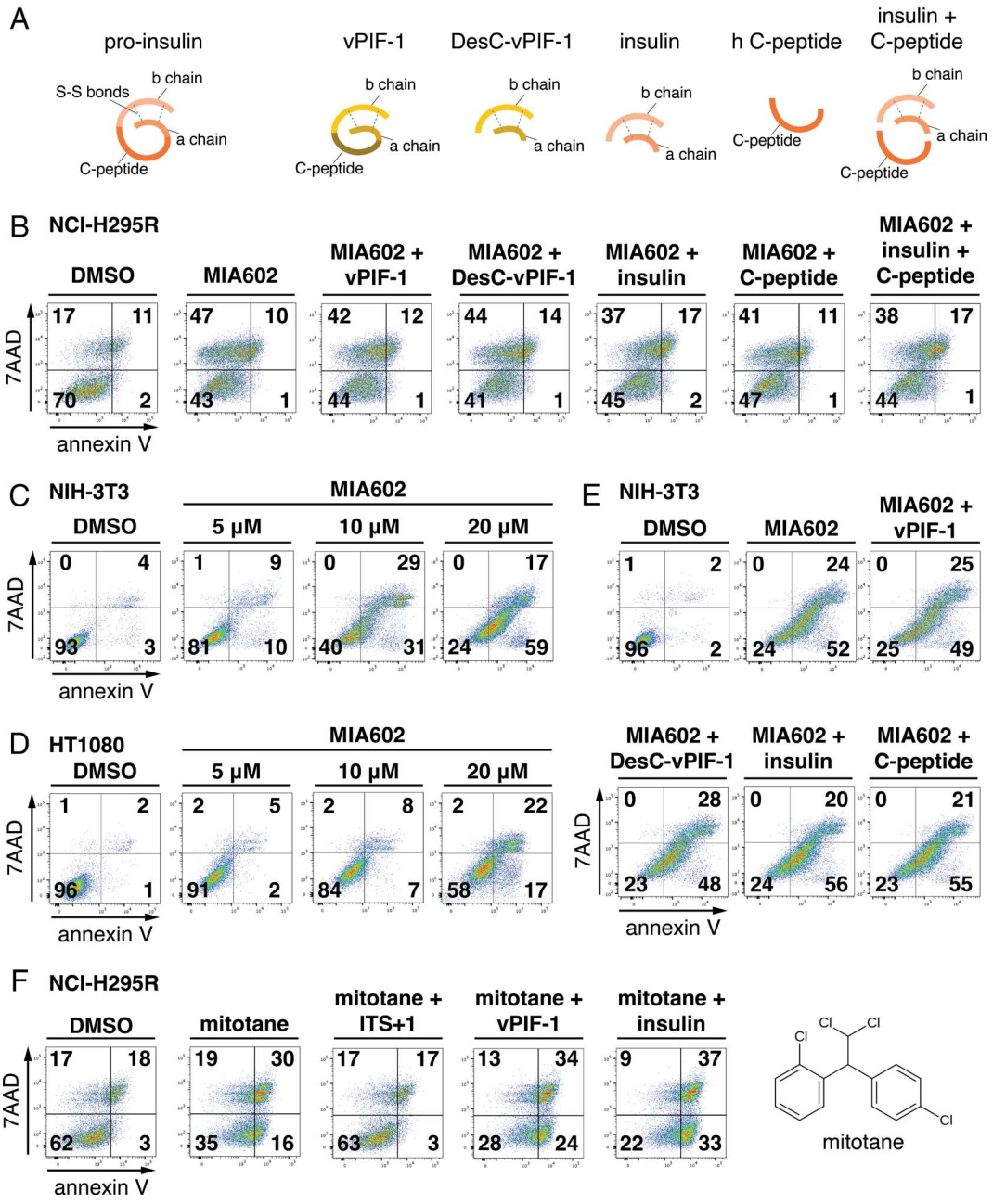

Fig. 2. The viral insulin, vPIF-1, does not prevent death induced by GHRH antagonists. (*A*) Cartoon showing a simplified version of the different chains composing the human and the viral insulin. (*B*) NCI-H295R cells were treated with the GHRH antagonist, MIA602 (10 µM), for 24 h and cotreated with 1 µM of vPIF-1, DesC-vPIF-1, human insulin, or human C-peptide. The combination of human insulin and C-peptide did not affect the MIA602-induced necrosis. Annexin V/7ADD positivity was assessed by FACS analysis. (*C*) NIH-3T3 and (*D*) HT1080 cells were challenged with different concentrations of MIA602 to investigate their sensitivity to this compound. Annexin V/7ADD positivity was assessed by FACS analysis. (*E*) NIH-3T3 cells were treated with MIA602 (10 µM) for 24 h and cotreated with 1 µM of vPIF-1, DesC-vPIF-1, human insulin, or human C-peptide and investigated by FACS analysis. (*F*) NCI-H295R cells were treated with 50 µM mitotane for 6 h. The presence of ITS+1 blocked this type of necrosis, but not vPIF-1 (1 µM) or human insulin (1 µM). All primary FACS data shown are representative examples of at least three independent experiments.

We decided to investigate the antiferroptotic activity of vPIF-1 in more detail. To this end, we systematically investigated its effects on cells treated with the known four classes of ferroptosis inducers (FINs), as well as the thioredoxin reductase inhibitor, ferroptocide (referred to as FTC) in HT1080 cells. Type I FINs, such as erastin, inhibit the glutamate-cystine antiporter system Xc-minus and thereby deplete the cells of glutathione (GSH) (28, 29), an essential cofactor of GPX4. Erastin-induced ferroptosis was inhibited by Fer-1 and vPIF-1, but not by DesC-vPIF-1, human insulin, or the human C-peptide (*SI Appendix*, Fig. S3*A*). Similarly, the vPIF-1-mediated protection from ferroptosis induced by the type II FIN RSL3 required the viral C-peptide as DesC-vPIF-1 failed to inhibit cell death in this assay (Fig. 4*A*), and vPIF-1 again exhibited potent antiferroptotic activity. We found similar patterns for the type III FIN FIN56 (*SI Appendix*, Fig. S3*B*) and the type IV FIN FINO2 (*SI Appendix*, Fig. S3*C*). In all cases, vPIF-1 protected from ferroptosis as potently as Fer-1, but DesC-vPIF-1 failed to rescue the HT1080 cells. Finally, to test an independent form of regulated lipid peroxidation, we investigated the thioredoxin reductase inhibitor FTC. As demonstrated in Fig. 4*B*, vPIF-1, but not Des-vPIF-1, human insulin, or the human C-peptide reversed FTC-induced necrosis. We confirmed the specificity of these results by testing RSL3-, FINO2-, and FTC-induced cell death in NCI-H295R cells with similar results (*SI Appendix*, Fig. S4 *A*–*C*).

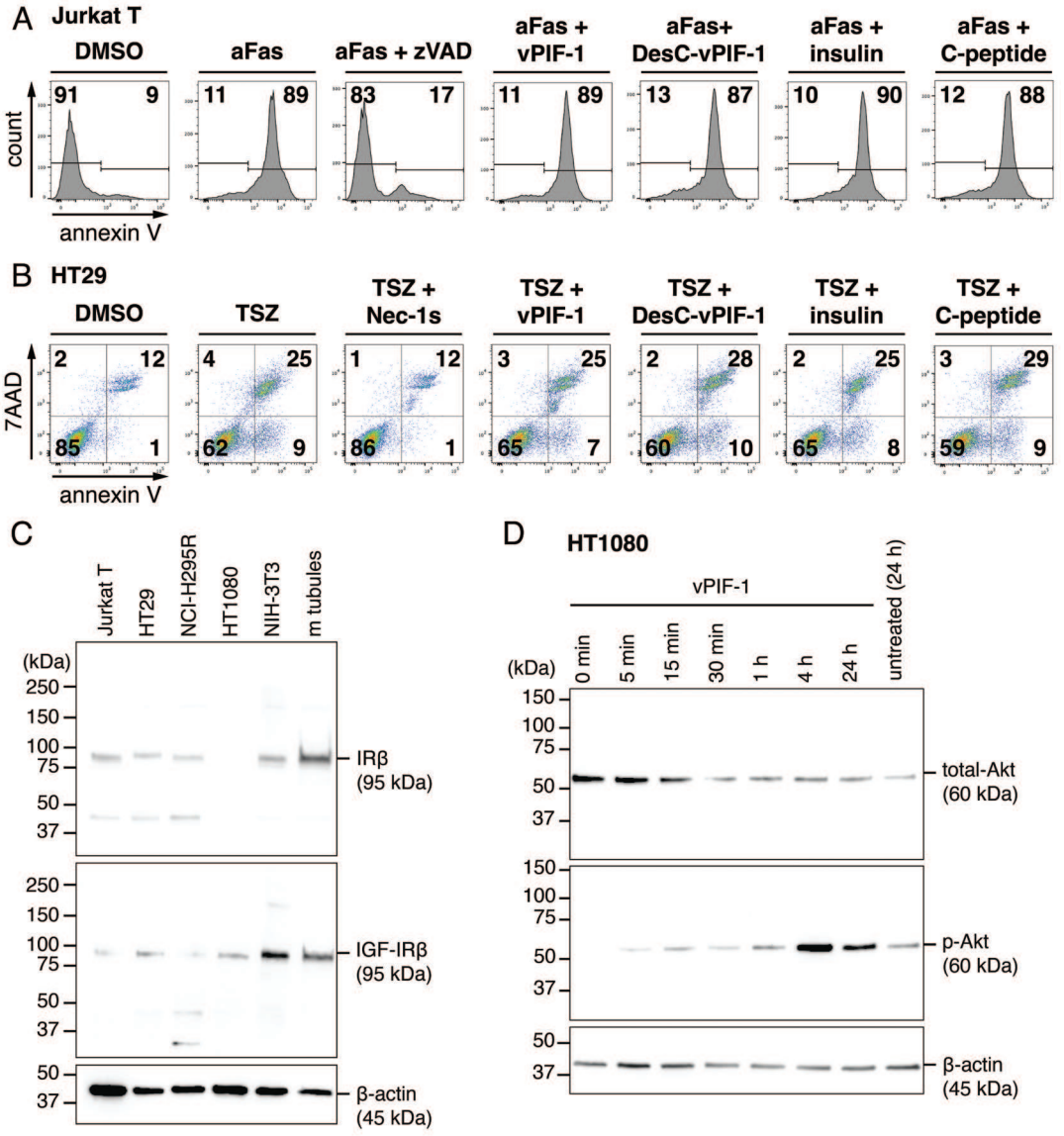

Fig. 3. The presence of the viral C-peptide does not affect apoptosis, necroptosis, or MIA602-induced necrosis. (*A*) Jurkat T cells were challenged to undergo apoptosis via anti-Fas (CD95) treatment (100 ng/mL) for 6 h. zVAD-fmk (20 μM) served as the protection control. None of the different types of insulin molecules (1 μM) were able to prevent apoptosis in this experimental setup. Annexin V positivity was assessed with FACS analysis. (*B*) HT29 cells were used to induce necroptosis by TNFα (20 ng/mL), smac mimetics (1 μM), and zVAD-fmk (20 μM) (referred to as TSZ) for 6 h, while Nec-1s (10 μM) served as the protection control. Cotreatment of the cells with 1 μM of vPIF-1, DesC-vPIF-1, human insulin, or human C-peptide did not prevent the induction of necroptosis. Annexin V/7ADD positivity was assessed with FACS analysis. The primary FACS data shown are representative examples of at least three independent experiments. (*C*) Assessment of the IRβ and type I IGF-IRβ in different cell lines as indicated and freshly isolated male renal tubules by western blot analysis. β-actin serves as a loading control. (*D*) HT1080 cells were treated with 1 μM of vPIF-1 for different time points. Cells were collected, the pellets were lysed, and Akt and phospho-Akt (p-Akt) were assessed via western blot analysis. An increase in the expression of p-Akt, as well as a decrease in the expression of Akt, can be noticed upon longer treatment with vPIF-1. Untreated HT1080 cells collected at 24 h served as a control. β-actin serves as a loading control.

To assess the mechanism of the antiferroptotic features of vPIF-1, we employed the cell-free FENIX lipid peroxidation inhibition assay [see *Materials and Methods* for details (30)]. Therein, the lipophilic radical initiator, DTUN, is used to initiate liposomal phospholipid peroxidation, which can be indirectly monitored by the corresponding oxidation of the added fluorophore STY-BODIPY. We detected a dose-dependent suppression of STY-BODIPY oxidation in the presence of vPIF-1, suggesting that it can inhibit lipid peroxidation as a radical-trapping antioxidant (RTA) (Fig. 4*C*). In contrast, DesC-vPIF-1, human insulin, and C-peptide showed no such effect (Fig. 4*C*). While the activity of vPIF-1 is clearly weaker than the Fer-1-positive control (consistent with the dose–response curve in Fig. 1*B*), it is clear that it can act as an RTA.

To test lipid peroxidation in a cellular assay, we investigated effects of the viral peptides on BODIPY 581/591 C11 positivity. As demonstrated in Fig. 4*D*, the ratio of FITC/PE channels showed a total shift of the RSL3- and vPIF-1-treated HT1080 cells similar to the vehicle control. DesC-vPIF-1, human insulin, and C-peptide failed to reduce the BODIPY oxidization upon RSL3 treatment. Similar results were obtained upon treatment of the cells with FTC (Fig. 4*E*). Collectively, these findings inevitably provide strong lines of evidence indicating the requirement of the vPIF-1 C-peptide for viral inhibition of ferroptosis and FTC-induced lipid peroxidation. Additionally, the mechanism of action of vPIF-1 is most likely mediated, at least partially, by its RTA activity. This set of experiments shows antiferroptosis activity in a virally encoded peptide.

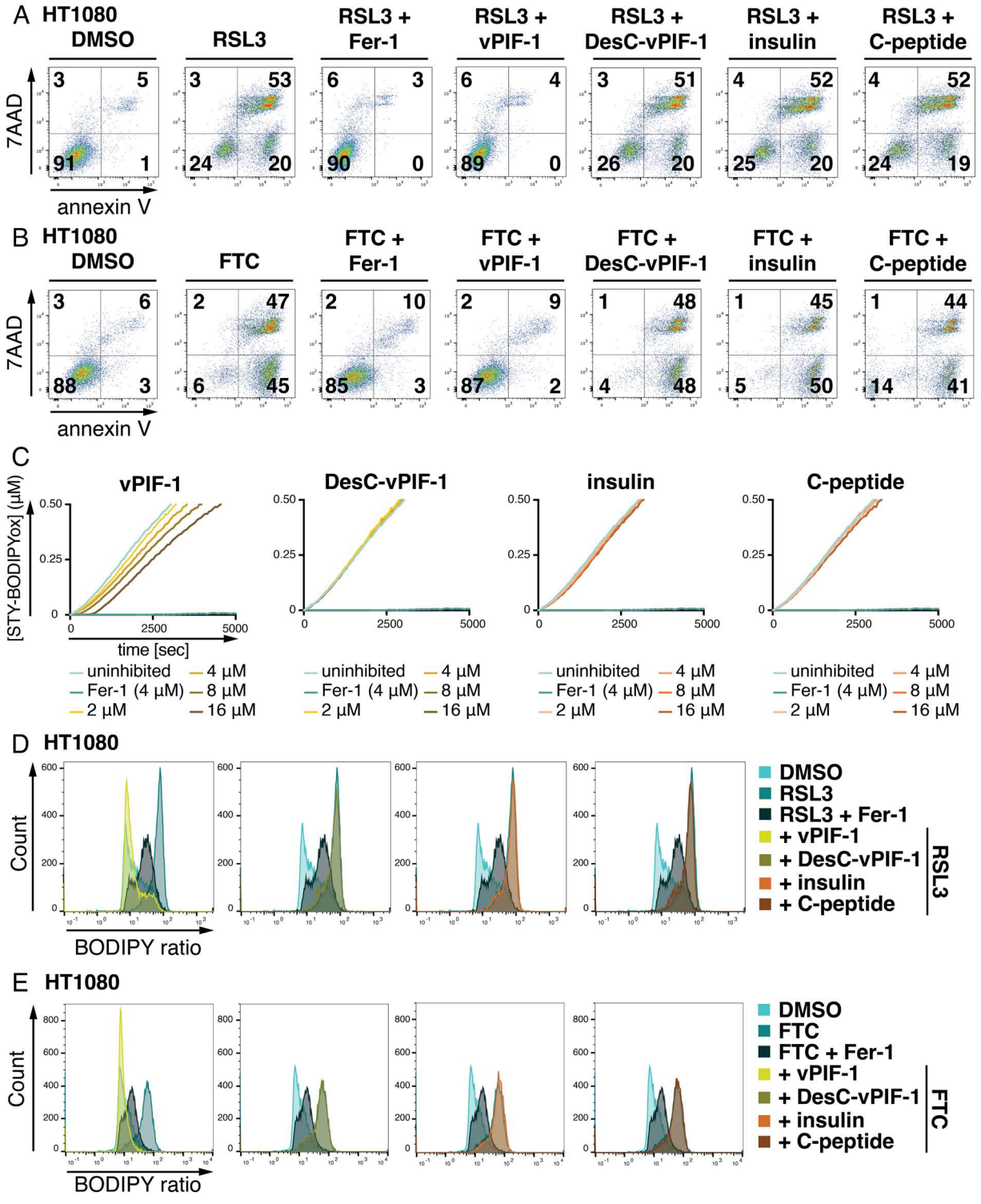

Fig. 4. The presence of the viral C-peptide in vPIF-1 provides it with RTA activity. (*A*) HT1080 cells were treated with type II FIN RSL3 (1.13 μM) for 6 h and (*B*) the thioredoxin inhibitor FTC (10 μM) for 6 h. For all experiments, cells were cotreated with 1 μM of vPIF-1, DesC-vPIF-1, human insulin, or human C-peptide. Annexin V/7ADD positivity was assessed with FACS analysis. All primary FACS data shown are representative examples of at least three independent experiments. (*C*) FENIX assay, a cell-free liposomal system, was employed to assess the RTA activity of vPIF-1, DesC-vPIF-1, human insulin, or human C-peptide. The assay revealed a dose-dependent delay in STY-BODIPY oxidation (an RTA feature) upon vPIF-1 treatment, while DesC-vPIF-1, human insulin, or human C-peptide showed no such activity. Fer-1 (4 μM) served as a positive control, displaying near-to-complete suppression of STY-BODIPY oxidation. (*D*) BODIPY 581/591 was used to stain HT1080 cells undergoing ferroptosis for 2 h via RSL3 (1.13 μM) or (*E*) necrotic cell death via FTC. Cells were cotreated with 1 μM of vPIF-1, DesC-vPIF-1, human insulin, or human C-peptide, and oxidization of BODIPY 581/591 was assessed by flow cytometry (data represent the ratio of the green and red channels). Fer-1 served as the protection control that shifts the histogram toward DMSO-treated cells. Note that vPIF-1 potently prevents the RSL3-induced shift.

Discussion

VILPs are approximately 200 to 500-fold less effective in triggering IR or IGF-1 receptors compared to their endogenous ligands (1). This notion prompted us to investigate insulin-independent functions of the LCDV-1-encoded VILP. There is much evidence for viruses to evade RCD programs to avoid clearance of the virus from infected cells. However, we did not observe this molecule to

affect apoptosis or necroptosis, the two best studied cell death pathways for viral defense. While it appeared clear to us that pyroptosis emerged as an antibacterial and inflammasome-dependent pathway, the role of ferroptosis had not been studied. We therefore tested the VILP in ferroptosis assays and observed an almost complete protection from ferroptosis induced by all FINs tested. Consequently, we suggest that this viral protein be named "vPIF-1." This study reports on a virally encoded protein that functions as an inhibitor of ferroptosis.

Iridoviridae infect fish, and fish have served as model systems for ferroptosis research. In essence, a particular feature of ferroptosis is cell death propagation between individual cellular compartments. Zebrafish fins are extraordinarily sensitive to ferroptosis and have been identified as a prototype example of this ferroptotic feature (31). In humans, the most sensitive cells to ferroptosis are renal tubules (25, 32) and adrenal cells (13, 33, 34). It remains to be investigated how epithelial layers of cells, upon viral infection, become particularly sensitive to ferroptosis, or if and how viruses may evade noncell autonomous cell death. Indeed, we have recently hypothesized that kidney tubular ferroptosis might allow regeneration of tissues (35). This might also be a favorable outcome to the host following viral infection. Along these lines, the recently identified ferroptosis-mediated inhibition of dendritic cell cross presentation (36) and the immunosuppressive features of ferroptotic polymorphonuclear cells (37) might actively inhibit the adaptive immune system. Future experiments will need to focus on the cell death–dependent outcome of epithelial tissues following viral infection.

Materials and Methods

Please refer to *SI Appendix, Materials and Methods* for further details.

Cell Death Assays. Ferroptosis was induced using established FINs: Type I FIN: erastin (Sigma Aldrich), type II FIN: RSL3 (Selleckchem), type III FIN: FIN56 (Sigma Aldrich), and type IV FIN: FINO2 (Cayman Chemical). Necrosis was induced as previously described by the thioredoxin reductase inhibitor FTC (38). Apoptosis was induced by treatment of Jurkat T cells with the antibody against Fas (100 ng/mL anti-Fas, Merk Millipore), while necroptosis was induced by treatment of HT29 cells with 20 ng/mL TNFα (BioLegend), 1 μM Birinapant (an SMAC mimetics inhibitor, ChemieTek), and 20 μM zVAD-fmk (BD Biosciences) (referred to as TSZ treatment). Cells were seeded in six-well plates. Unless otherwise indicated, we used 5 μM erastin, 1.13 μM RSL3, 10 μM FIN56, 10 μM $FINO_2$, and 10 μM FTC. After indicated time points, the cells were collected and prepared for flow cytometry, immunoblotting, or BODIPY 581/591 assay.

Flow Cytometry. Cells were harvested, and the pellets were washed twice in PBS and stained with 5 μL 7-AAD (BD Biosciences) and 5 μL annexin-V-FITC (BD Biosciences) added to 100 μL annexin-V binding buffer solution (BD Biosciences). After 15 min, the cells were recorded on the Fortessa LSRII with the FACS Diva 6.1.1 software (BD Biosciences) and subsequently analyzed with the FlowJo v10 software (Tree Star). The flow cytometry procedure was supported by the Flow Cytometry Core Facility of the CMCB Technology Platform at TU Dresden.

Western Blotting. Cells were lysed in ice-cold 50 mM Tris-HCl, pH 7.5, 150 mM NaCl, 1% NP-40, 5 mM EDTA supplemented with PhosSTOP™ (Merck), cOmplete™ (Merck), and 1 mM phenylmethylsulfonyl fluoride (PMSF) for 30 min on ice. To determine protein levels, the cells were lysed in ice-cold 50 mM Tris-HCl, pH 8, 150 mM NaCl, 0.5% sodium deoxychelate, 0.1% SDS supplemented with PhosSTOPTM (Merck), cOmpleteTM (Merck), 1 mM PMSF, and 100mM octyl-β-D-glucopyranoside for 30 min on ice. Insoluble material was removed by centrifugation (14,000 g, 30 min, 4 °C). Protein concentration was determined using a commercial BCA assay kit according to the instructions of the manufacturer (Thermo Fisher). Equal amounts of protein (typically 25 μg per lane) were resolved on a 4 to 15% gradient SDS/PAGE gel and transferred to a PVDF membrane (BIO-RAD). After blocking for 1 h at room temperature, incubation with primary antibody was performed at 4 °C over night. Primary antibodies against IRβ (Cell Signaling, #23413) and type I IGF receptor beta (IGF-IRβ) (Cell Signaling, #9750) were diluted 1:1,000 in 5% BSA (SERVA, # 9048-46-8). Primary antibodies against Akt (Cell Signaling, #9272), p-Akt (Cell Signaling, #9271), and β-actin (Cell Signaling, #3700S) were diluted 1:1,000 in fatty-free milk (Roth, # 68514-61-4). Secondary antibodies (anti-mouse, HRP-linked antibody, Cell Signaling, Cat# 7076S; anti-rabbit, HRP-linked antibody, Cell Signaling, Cat# 7074S) were applied at concentrations of 1:5,000. Proteins were then visualized by enhanced chemiluminescence (ECL; Amersham Biosciences).

FENIX Assay. Egg phosphatidylcholine liposomes (1.03 mM) [prepared as previously described by Li et al. (39)], STY-BODIPY (1.03 μM), and di-*tert*-undecyl hyponitrite (DTUN) (0.21 mM) in chelex-treated phosphate-buffered saline (cPBS) (12 mM phosphate, 150 mM NaCl, pH 7.4) were added to the wells of an Nunc black polypropylene round-bottomed 96-well microplate (195 μL). Using a 1 to 10 μL multichannel pipette, 5 μL of inhibitor solution in water (peptides) or DMSO (Fer-1) or vehicle only was then added to afford a final volume of 200 μL (final concentration of 1 mM egg-PC, 1 μM STY-BODIPY, 0.2 mM DTUN, and inhibitor varying between 2 and 16 μM). The reaction mixtures were manually mixed using a 100 to 300 μL multichannel pipette (set to 150 μL) and the microplate was inserted into a BioTek H1 Synergy microplate reader equilibrated to 37 °C and vigorously shook for 1 min followed by a 3.5-min delay. Fluorescence was then recorded (λ_{ex} = 488 nm; λ_{em} = 518 nm; gain = 60) every minute for 6 h.

Mice. Eight-to-twelve-week-old male mice were cohoused two to five mice/cage in IVCs in our facility at the Medizinisch-Theoretisches Zentrum (MTZ) at the Medical Faculty of the Technical University of Dresden (TU Dresden). All wild-type mice (C57Bl/6N) were initially provided by Charles River, at the age of 6 to 7 wk. All experiments were performed according to German animal protection laws and were approved by ethics committees and local authorities of Dresden (Germany).

Statistical Analysis. Statistical analyses were performed with Prism 9 (GraphPad software) using Student's *t* test or one-way ANOVA. Data were considered significant when $*P \le 0.05$, $**P \le 0.01$, $***P \le 0.001$, or $****P \le 0.0001$.

Data, Materials, and Software Availability. All study data are included in the article and/or *SI Appendix*.

ACKNOWLEDGMENTS. We would like to cordially thank Romy Opitz, Anne Pioch, and Monique Hoffmann for expert technical assistance. Work in the Linkermann Lab was funded by the Medical Clinic 3, University Hospital Carl Gustav Carus Dresden, Germany, and supported by the SFB-TRR205, SFB-TRR 127, SPP3206, BMBF (Bundesministerium für Bildung und Forschung, FERROPath consortium), and the international research training group 2251. This work was additionally supported by the German Research Foundation (Deutsche Forschungsgemeinschaft, DFG) (Heisenberg-Professorship to A.L., project number 324141047) and the Natural Sciences and Engineering Research Council of Canada (Discovery Grant to D.A.P., RGPIN-2022-05058). Further funding for this project was received by the transCampus initiative to S.R.B.

Author affiliations: [a]Division of Nephrology, Department of Internal Medicine III, University Hospital Carl Gustav Carus at the Technische Universität Dresden, 01307 Dresden, Germany; [b]Department of Chemistry and Biomolecular Sciences, University of Ottawa, Ottawa, ON K1N 6N5, Canada; [c]King's College London, British Heart Foundation Centre of Research Excellence, School of Cardiovascular and Metabolic Medicine & Sciences, WC2R 2LS London, United Kingdom; [d]Institute of Medical Virology, University of Zürich 8057, Zürich, Switzerland; [e]Department of Medicine III, University Hospital Carl Gustav Carus, Technische Universität Dresden, 01307 Dresden, Germany; [f]Veterans Affairs Medical Center, Miami, FL 33125; [g]Department of Pathology, Miller School of Medicine, University of Miami, Miami, FL 33150; [h]Division of Endocrinology, Department of Medicine, Miller School of Medicine, University of Miami, Miami, FL 33136; [i]Division of Medical Oncology, Department of Medicine, Miller School of Medicine, University of Miami, Miami, FL 33136; [j]Sylvester Comprehensive Cancer Center, Miller School of Medicine, University of Miami, Miami, FL 33136; [k]Diabetes and Nutritional Sciences, King's College London, WC2R 2LS London, United Kingdom; [l]Center for Regenerative Therapies, Technische Universität Dresden, 01307 Dresden, Germany; [m]Paul Langerhans Institute Dresden of Helmholtz Centre Munich at University Clinic Carl Gustav Carus of Technische Universität Dresden, Faculty of Medicine, 01307 Dresden, Germany; [n]Lee Kong Chian School of Medicine, Nanyang Technological University, 636921 Singapore, Singapore; and [o]Division of Nephrology, Department of Medicine, Albert Einstein College of Medicine, Bronx, NY 10461

1. E. Altindis *et al.*, Viral insulin-like peptides activate human insulin and IGF-1 receptor signaling: A paradigm shift for host-microbe interactions. *Proc. Natl. Acad. Sci. U.S.A.* **115**, 2461–2466 (2018).
2. K. Girdhar *et al.*, Viruses and metabolism: The effects of viral infections and viral insulins on host metabolism. *Annu. Rev. Virol.* **8**, 373–391 (2021).
3. B. Gorai, H. Vashisth, Structural models of viral insulin-like peptides and their analogs. *Proteins* **91**, 62–73 (2022).
4. D. M. Irwin, Viral Insulin/IGF-1-like peptides: Novel regulators of physiology and pathophysiology? *Endocrinology* **159**, 3659–3660 (2018).
5. M. Chrudinová *et al.*, Characterization of viral insulins reveals white adipose tissue-specific effects in mice. *Mol. Metab.* **44**, 101121 (2021).
6. F. Zhang, E. Altindis, C. R. Kahn, R. D. DiMarchi, V. Gelfanov, A viral insulin-like peptide is a natural competitive antagonist of the human IGF-1 receptor. *Mol. Metab.* **53**, 101316 (2021).
7. F. Moreau *et al.*, Interaction of a viral insulin-like peptide with the IGF-1 receptor produces a natural antagonist. *Nat. Commun.* **13**, 6700 (2022).
8. K. D. Kimura, H. A. Tissenbaum, Y. Liu, G. Ruvkun, daf-2, an insulin receptor-like gene that regulates longevity and diapause in Caenorhabditis elegans. *Science.* **277**, 942–946 (1997).
9. S. Nagata, K. Segawa, Sensing and clearance of apoptotic cells. *Curr. Opin. Immunol.* **68**, 1–8 (2021).
10. A. Linkermann, D. R. Green, Necroptosis. *N. Engl. J. Med.* **370**, 455–465 (2014).
11. P. Broz, P. Pelegrín, F. Shao, The gasdermins, a protein family executing cell death and inflammation. *Nat. Rev. Immunol.* **20**, 143–157 (2020).
12. B. R. Stockwell *et al.*, Ferroptosis: A regulated cell death nexus linking metabolism, redox biology, and disease. *Cell* **171**, 273–285 (2017).
13. A. Belavgeni *et al.*, Exquisite sensitivity of adrenocortical carcinomas to induction of ferroptosis. *Proc. Natl. Acad. Sci. U.S.A.* **116**, 22269–22274 (2019).
14. P. Broz, V. M. Dixit, Inflammasomes: Mechanism of assembly, regulation and signalling. *Nat. Rev. Immunol.* **16**, 407–420 (2016).
15. W. J. Kaiser, J. W. Upton, E. S. Mocarski, Viral modulation of programmed necrosis. *Curr. Opin. Virol.* **3**, 296–306 (2013).
16. T. Komiyama, L. T. Quan, G. S. Salvesen, Inhibition of cysteine and serine proteinases by the cowpox virus serpin CRMA. *Adv. Exp. Med. Biol.* **389**, 173–176 (1996).
17. V. S. Goldmacher, vMIA, a viral inhibitor of apoptosis targeting mitochondria. *Biochimie* **84**, 177–185 (2002).
18. A. L. McCormick, Control of apoptosis by human cytomegalovirus. *Curr. Topics Microbiol. Immunol.* **325**, 281–295 (2008).
19. J. W. Upton, W. J. Kaiser, E. S. Mocarski, Cytomegalovirus M45 cell death suppression requires receptor-interacting protein (RIP) homotypic interaction motif (RHIM)-dependent interaction with RIP1. *J. Biol. Chem.* **283**, 16966–16970 (2008).
20. B. R. Stockwell, Ferroptosis turns 10: Emerging mechanisms, physiological functions, and therapeutic applications. *Cell* **185**, 2401–2421 (2022).
21. M. Conrad, J. P. Angeli, P. Vandenabeele, B. R. Stockwell, Regulated necrosis: Disease relevance and therapeutic opportunities. *Nat. Rev. Drug Discov.* **15**, 348–366 (2016).
22. O. Zilka *et al.*, On the mechanism of cytoprotection by ferrostatin-1 and liproxstatin-1 and the role of lipid peroxidation in ferroptotic cell death. *ACS Cent. Sci.* **3**, 232–243 (2017).
23. L. Sun *et al.*, Mixed lineage kinase domain-like protein mediates necrosis signaling downstream of RIP3 kinase. *Cell* **148**, 213–227 (2012).
24. J. P. Friedmann Angeli *et al.*, Inactivation of the ferroptosis regulator Gpx4 triggers acute renal failure in mice. *Nat. Cell Biol.* **16**, 1180–1191 (2014).
25. A. Linkermann *et al.*, Synchronized renal tubular cell death involves ferroptosis. *Proc. Natl. Acad. Sci. U.S.A.* **111**, 16836–16841 (2014).
26. R. Skouta *et al.*, Ferrostatins inhibit oxidative lipid damage and cell death in diverse disease models. *J. Am. Chem. Soc.* **136**, 4551–4556 (2014).
27. B. M. Burgering, P. J. Coffer, Protein kinase B (c-Akt) in phosphatidylinositol-3-OH kinase signal transduction. *Nature* **376**, 599–602 (1995).
28. S. J. Dixon *et al.*, Ferroptosis: An iron-dependent form of nonapoptotic cell death. *Cell* **149**, 1060–1072 (2012).
29. N. Yagoda *et al.*, RAS-RAF-MEK-dependent oxidative cell death involving voltage-dependent anion channels. *Nature* **447**, 864–868 (2007).
30. R. Shah, L. A. Farmer, O. Zilka, A. T. M. Van Kessel, D. A. Pratt, Beyond DPPH: Use of fluorescence-enabled inhibited autoxidation to predict oxidative cell death rescue. *Cell Chem. Biol.* **26**, 1594–1607.e1597 (2019).
31. A. Katikaneni *et al.*, Lipid peroxidation regulates long-range wound detection through 5-lipoxygenase in zebrafish. *Nat. Cell Biol.* **22**, 1049–1055 (2020).
32. A. von Mässenhausen *et al.*, Dexamethasone sensitizes to ferroptosis by glucocorticoid receptor-induced dipeptidase-1 expression and glutathione depletion. *Sci. Adv.* **8**, eabl8920 (2022).
33. W. Tonnus *et al.*, The role of regulated necrosis in endocrine diseases. *Nat. Rev. Endocrinol.*, inpress.
34. I. Weigand *et al.*, Active steroid hormone synthesis renders adrenocortical cells highly susceptible to type II ferroptosis induction. *Cell Death Dis.* **11**, 192 (2020).
35. F. Maremonti, C. Meyer, A. Linkermann, Mechanisms and models of kidney tubular necrosis and nephron loss. *J. Am. Soc. Nephrol.* **33**, 472–486 (2022).
36. B. Wiernicki *et al.*, Excessive phospholipid peroxidation distinguishes ferroptosis from other cell death modes including pyroptosis. *Cell Death Dis.* **11**, 922 (2020).
37. R. Kim *et al.*, Ferroptosis of tumour neutrophils causes immune suppression in cancer. *Nature* **612**, 338–346 (2022).
38. E. Llabani *et al.*, Diverse compounds from pleuromutilin lead to a thioredoxin inhibitor and inducer of ferroptosis. *Nat. Chem.* **11**, 521–532 (2019).
39. B. Li *et al.*, Besting vitamin E: Sidechain substitution is key to the reactivity of naphthyridinol antioxidants in lipid bilayers. *J. Am. Chem. Soc.* **135**, 1394–1405 (2013).